Manipulability of Leader-Follower Networks with the Rigid-Link Approximation

Hiroaki Kawashima [a], Magnus Egerstedt [b]

[a] *Graduate School of Informatics, Kyoto University, Yoshida-honmachi, Sakyo, Kyoto 6068501, Japan*

[b] *School of Electrical and Computer Engineering, Georgia Institute of Technology, Atlanta, GA 30308, USA*

Abstract

This paper introduces the notion of *manipulability* to mobile, multi-agent networks as a tool to analyze the instantaneous effectiveness of injecting control inputs at certain, so-called leader nodes in the network. Effectiveness is interpreted to characterize how the movements of the leader nodes translate into responses among the remaining follower nodes. This notion of effectiveness is a function of the interaction topologies, the agent configurations, and the particular choice of inputs used to influence the network. In fact, classic manipulability is an index used in robotics to analyze the singularity and efficiency of configurations of robot-arm manipulators. To define similar notions for leader-follower networks, we use a rigid-link approximation of the follower dynamics and, under this assumption, we prove that the instantaneous follower velocities can be uniquely determined from that of the leaders', which allows us to define a meaningful and computable manipulability index for the leader-follower networks. This paper examines the property of the proposed index in simulation and with real mobile robots, and demonstrates how the index can be used to find effective interaction topologies.

Key words: Multi-agent systems, rigidity theory, networked mobile robots.

1 Introduction

Consider a system consisting of multiple mobile units, connected together through an information-exchange network, where the agents use the information-exchange network for their coordination. If the movement of a particular agent is thought of as the input to the system, one can ask a number of questions pertaining to the input's effect on the rest of the system, including: (1) What is the set of states reachable under this control structure?, (2) How "effective" is the control input in terms of the network's response?, and (3) How can we design or adaptively improve the network topology to render it more "amenable" to the control inputs?

Significant progress has been made by the community over the last decade trying to understand networked dynamical systems in general, e.g., [9,11,26,19,17]. A number of decentralized mobility and coordination algorithms have been used successfully for achieving and maintaining formations [12,21], for covering areas [3,16], or for securing and tracking boundary curves [18,29], just to name a few.

Email addresses: `kawashima@i.kyoto-u.ac.jp` (Hiroaki Kawashima), `magnus@gatech.edu` (Magnus Egerstedt).

For such mobile networks with a given set of interaction laws, it is sometimes desirable to be able to influence the agents by injecting external control signals. One way in which such control authority can be achieved is by injecting the control signals at particular input nodes, and such an organization is referred to as a leader-follower network. In this paper, we follow this route, and consider the situation where each follower agent is moving based solely on locally available information, while the leaders' movements are dictated by the external control input. In fact, a large body of work has emerged concerning how to control such networks. Examples include optimal control [17], containment control [4,10], and formation control [7,20].

Question (1) in the first paragraph is intimately linked to the controllability properties of such leader-follower networks, which has been investigated, for example, in [23,25]. Controllability, however, is a point-to-point property in the sense that it characterizes what states are reachable from one another. In this paper, we ignore this question and focus instead on a more modest issue, namely Question (2), i.e., the question of how "effective" the control input is over a short time horizon. This is not a controllability question but rather it connects the input signals to instantaneous system responses.

(a) More effective   (b) Less effective
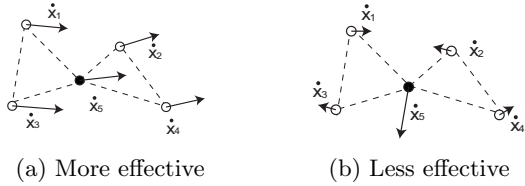
Fig. 1. Effectiveness is defined using the ratio between the norm of the followers' velocities (response) and that of the leader's velocity (input) ($N_\ell = 1$ case). The filled circle x_5 is the leader and dashed lines depict interconnections of agents.

In particular, this paper considers a leader-follower network in which each follower tries to maintain given desired distances from its neighbors so as to achieve a rigid/non-rigid formation. Under such situations, instantaneous "effectiveness" of external inputs is particularly important in several applications, such as in emerging area of human-swarm interaction. While there are a number of ways humans interact with a large collection of robots (e.g., [5,15]), we are interested in an approach that a human operator controls the designated robot in the network as the leader. What is critical here is that humans are crucially sensitive to how intuitive his/her inputs are propagated through the network and effectively manipulate the movements of the followers [6]. However, it is still not well-understood how such instantaneous system responses should be measured.

To address the notion of input "effectiveness", we borrow the notion of *manipulability*, and transfer it to leader-follower networks as a tool to analyze the instantaneous effectiveness of the leader inputs to the network under given agent configurations and network topologies (Fig. 1). In robotics, the manipulability indices have been proposed as means for analyzing the singularity and efficiency of particular configurations when controlling robot-arm manipulators [27,1,2]. And, while the original manipulability indices are based on taking the Jacobian of the kinematic relation between the input angular velocities of the joints and the generated velocities of the end-effectors, leader-follower network "links" are not rigid in the same way. As such, we are forced to approximate the interaction dynamics in order to be able to define manipulability in terms of the *instantaneous* relation between the leaders' and the followers' velocities.

Initial work along these lines was done in [13], and here we extend this contribution by establishing novel properties of the proposed index, applying these concepts to real mobile robots, and demonstrating how it can be used to find effective topologies. In fact, the contributions in this paper are twofold. First, we show how the dynamics of leader-follower networks can be approximated by assuming all the edges as rigid links when the followers move fast enough to maintain given desired distances. Second, we introduce the notion of manipulability to leader-follower networks as the index of how leaders' movements have impacts on followers' movements.

2 Leader-Follower Networks

2.1 Multi-Agent Networks with Leaders and Followers

Let $x_i(t) \in \mathbb{R}^d$ ($i = 1, ..., N$) be the state of agent i at time t. [1] Then the overall state (configuration) of the network is given by $x(t) = [x_1^T(t), ..., x_N^T(t)]^T \in \mathbb{R}^{Nd}$. Now, assume that these agents are arranged over an information-exchange network, with N_ℓ out of N agents assigned to be leaders, whose movements are considered to be the input to the overall system. The remaining $N_f = N - N_\ell$ agents are referred to as followers, each of which obeys a given control law based solely on locally available information.

In this paper, we consider the situation where the interaction dynamics are defined through pairwise interactions. We say that when follower agents i and j are *connected*, they can share relative state information, and their pairwise control task is to maintain the distance $\|x_i - x_j\|$ to a pre-specified, positive value d_{ij}. If one of the agents in a connected pair is a leader agent and the other is a follower, then the follower dynamics is designed so as to maintain the distance.

Using a graph representation of this interaction structure, the agents are described by nodes $\mathsf{V} = \{\mathsf{v}_1, ..., \mathsf{v}_N\}$ and the connections between agents become edges $\mathsf{E} \subseteq \mathsf{V} \times \mathsf{V}$, where the number of edges is $M = |\mathsf{E}|$ (the cardinality of E). Then, the overall network is described by the graph $\mathsf{G} = (\mathsf{V}, \mathsf{E})$. In this paper, we mostly consider networks whose underlying graphs are undirected (the interconnections are symmetric), static, and connected. [2]

2.2 Leader and Follower Assignments

To explicitly denote the designation of nodes as either being leaders or followers, we introduce the following notation: Let $\ell : \{1, ..., N_\ell\} \to \{1, ..., N\}$ be an injective function whose image, $\ell(\{1, ..., N_\ell\}) = \{\ell(i)|i = 1, ..., N_\ell\}$, is the set of leaders indices. Let δ_i be a vector whose i-th entry is 1 and all the remaining entries are 0s. Using the $N \times N_\ell$ matrix $\Delta_\ell \triangleq [\delta_{\ell(1)}, ..., \delta_{\ell(N_\ell)}]$, we can define a leader indicator vector as $\hat{\delta}_\ell \triangleq \Delta_\ell \mathbf{1}_{N_\ell}$, where $\mathbf{1}_p$ is a p-dimensional column vector with 1s in all its entries. This indicator vector, $\hat{\delta}_\ell$ contains the indices of the leaders and in a similar way, we can define a corresponding follower indicator vector by defining the

---

[1] This could, for instance, be the position of the mobile agent with $d = 2$ or $d = 3$. In this paper, we primarily address the $d = 2$ case – especially in examples – and use terms such as "movement" and "velocity" to reflect this particular example while most of the discussion holds in arbitrary dimensions.

[2] The assumption about static networks will only be used instantaneously, i.e., over short time-horizons. During the actual evolution of the system, the edge set will, however, be allowed to vary over time, e.g., as a function of inter-agent distances.

injective function $f : \{1, ..., N_f\} \rightarrow \{1, ..., N\}$ such that $\ell(\{1, ..., N_\ell\}) \cup f(\{1, ..., N_f\}) = \{1, ..., N\}$ and the matrix $\Delta_f \triangleq [\delta_{f(1)}, ..., \delta_{f(N_f)}]$. As a consequence, we have that $\hat{\delta}_f \triangleq \Delta_f \mathbf{1}_{N_f}$ becomes the follower indicator vector.

Using this notation, we can define the permutation matrix $P = [\Delta_f | \Delta_\ell]$, satisfying $P^T P = P P^T = I_N$, where I_p denotes the $p \times p$ identity matrix. Besides, relations such as $\Delta_\ell \Delta_\ell^T = \text{Diag}(\hat{\delta}_\ell)$, $\Delta_\ell^T \Delta_\ell = I_{N_\ell}$, $\Delta_\ell^T \mathbf{1}_N = \mathbf{1}_{N_\ell}$, and $\hat{\delta}_\ell^T \mathbf{1}_N = N_\ell$ will be used throughout the paper, where $\text{Diag}(a)$ is the diagonal matrix whose diagonal entries is the vector a.

Now, the states of the leaders and followers can be grouped together and denoted by vectors $x_\ell(t) \in \mathbb{R}^{N_\ell d}$ and $x_f(t) \in \mathbb{R}^{N_f d}$, respectively:

$$
\begin{aligned}
x_\ell(t) &= [x_{\ell(1)}^T(t), ..., x_{\ell(N_\ell)}^T(t)]^T = (\Delta_\ell^T \otimes I_d) x(t), \\
x_f(t) &= [x_{f(1)}^T(t), ..., x_{f(N_f)}^T(t)]^T = (\Delta_f^T \otimes I_d) x(t),
\end{aligned} \tag{1}
$$

and

$$
x(t) = (\Delta_\ell \otimes I_d) x_\ell(t) + (\Delta_f \otimes I_d) x_f(t), \tag{2}
$$

where $\otimes$ denotes the Kronecker product.

Example 2.1 *The functions $\ell(i) = N_f + i$ $(i = 1, ..., N_\ell)$ and $f(i) = i$ $(i = 1, ..., N_f)$ assign the last indices of $\{1, ..., N\}$ to the leaders. Thus, $\Delta_f = [I_{N_f}|0]^T$, $\Delta_\ell = [0|I_{N_\ell}]^T$, and $x = [x_f^T, x_\ell^T]^T$, where $x_f = [x_1^T, ..., x_{N_f}^T]^T$ and $x_\ell = [x_{N_f+1}^T, ..., x_N^T]^T$. (See Fig 1 for $N_f = 4, N_\ell = 1$ case.)*

2.3 Edge-Tension Energies

To formulate the followers' dynamics, we use a general, energy-based definition (e.g., [17]), which enables agents to achieve a distance-based formation. Let

$$
\mathcal{E}(x) = \frac{1}{2} \sum_{i=1}^{N} \sum_{j=1}^{N} \mathcal{E}_{ij}(x_i(t), x_j(t)) \tag{3}
$$

be the edge-tension energy, which is the summation of

$$
\mathcal{E}_{ij}(x_i, x_j) = \begin{cases} \frac{1}{2} \left(e_{ij}(||x_i - x_j||) \right)^2 & \{\mathsf{v}_i, \mathsf{v}_j\} \in \mathsf{E} \\ 0 & \{\mathsf{v}_i, \mathsf{v}_j\} \notin \mathsf{E}, \end{cases} \tag{4}
$$

where $e_{ij} : \mathbb{R}_+ \rightarrow \mathbb{R}$ is a strictly increasing, twice differentiable function such that $e_{ij}(d_{ij}) = 0$ $(d_{ij} > 0)$ and $e'_{ij}(d_{ij}) \neq 0$, where $e'_{ij}(z) \triangleq \frac{de_{ij}(z)}{dz}$. We also assume that connected agents do not have identical states, i.e., we assume that $||x_i - x_j|| > 0$ $\forall \{\mathsf{v}_i, \mathsf{v}_j\} \in \mathsf{E}$.

An example of a typical choice for the function e_{ij} is (see [17] and the references therein)

$$
e_{ij}(||x_i - x_j||) = c_{ij}(||x_i - x_j|| - d_{ij}), \tag{5}
$$

where the constant $c_{ij}(> 0)$ is a weight on edge $\{\mathsf{v}_i, \mathsf{v}_j\}$.

The reason for formulating these edge-tensions is that they can be used to derive distributed interaction laws for the followers in a straightforward and systematic manner, which is the topic of the next section.

2.4 Agent Dynamics

Given leaders' movements as the input to the network:

$$
\dot{x}_\ell(t) = [\dot{x}_{\ell(1)}^T(t), ..., \dot{x}_{\ell(N_\ell)}^T(t)]^T = u_\ell(t), \tag{6}
$$

we define the dynamics of the followers such that each of the followers tries to minimize their related parts of the edge-tension energy (3) in a decentralized manner through a gradient descent direction:

$$
\dot{x}_i(t) = - \sum_{j \in \mathcal{N}(i)} \frac{\partial \mathcal{E}_{ij}(x_i(t), x_j(t))}{\partial x_i}^T , \quad i \in f(\{1, ..., N_f\}), \tag{7}
$$

where $\mathcal{N}(i) = \{j \in \{1, ..., N\} \mid \{\mathsf{v}_i, \mathsf{v}_j\} \in \mathsf{E}\}$ is the neighbor set of agent i. That is, the dynamics of the followers is designed such that each of the followers tries to maintain the desired distances to adjacent agents. Using the facts that $\mathcal{E}_{ij} = \mathcal{E}_{ji}$ and $\frac{\partial \mathcal{E}}{\partial x_i} = \frac{1}{2} \sum_{j \in \mathcal{N}(i)} \left(\frac{\partial \mathcal{E}_{ij}}{\partial x_i} + \frac{\partial \mathcal{E}_{ji}}{\partial x_i} \right)$, the dynamics of overall followers in the network can be described by

$$
\dot{x}_f(t) = [\dot{x}_{f(1)}^T(t), ..., \dot{x}_{f(N_f)}^T(t)]^T = -\frac{\partial \mathcal{E}(x)}{\partial x_f}^T . \tag{8}
$$

Therefore, using this dynamics, the followers try to decrease (locally) the total energy (3) since $\dot{\mathcal{E}} = \frac{\partial \mathcal{E}}{\partial x_f} \dot{x}_f + \frac{\partial \mathcal{E}}{\partial x_\ell} \dot{x}_\ell = -||\frac{\partial \mathcal{E}}{\partial x_f}||^2 + \frac{\partial \mathcal{E}}{\partial x_\ell} \dot{x}_\ell$. In particular, if the leaders are not moving (i.e., $\dot{x}_\ell = 0$), the energy will not be increased (decreased in many situations) by the followers, thus serving as a prime candidate for a Lyapunov function when designing formation controllers.

Since the edge-tensions are are functions of the relative distances $||x_i - x_j||$, it follows that

$$
\frac{\partial \mathcal{E}_{ij}(x_i, x_j)}{\partial x_i} = w_{ij}(||x_i - x_j||)(x_i - x_j)^T,
$$

where $w_{ij}(z) \triangleq \{e_{ij}(z)e'_{ij}(z)\}/z$, with $z > 0$. Thus, (7) becomes a state-dependent, weighted consensus equation [17].

In other words, let $D \in \mathbb{R}^{N \times M}$ be the incidence matrix of graph G with an arbitrary but consistent assignment of the orientation on the edges. Let $W(x) \in \mathbb{R}^{M \times M}$ be the diagonal weight matrix, where $[W(x)]_{kk} = w_{i_k j_k}(||x_{i_k} - x_{j_k}||)$, where i_k and j_k are the agents connected by edge k. Then, the weighted graph Laplacian of G becomes $L_w(x) = DW(x)D^T \in \mathbb{R}^{N \times N}$. As a consequence, if all agents were followers, the interaction laws become $\dot{x} = -(L_w \otimes I_d)x$. Therefore, noting the relation $(X \otimes I_d)(Y \otimes I_d) = XY \otimes I_d$ and using (1), we can rewrite (8) on ensemble form as

$$\dot{x}_f(t) = -((\Delta_f^T L_w) \otimes I_d)x(t).$$

By adding the leaders to the formulation, the dynamics of all the agents combined become

$$\dot{x} = -((\text{Diag}(\hat{\delta}_f)L_w) \otimes I_d)x + (\Delta_\ell \otimes I_d)u_\ell, \quad (9)$$

where we note that (9) is a nonlinear system since L_w is a function of x.

3 Manipulability of Leader-Follower Networks

One of the most well-studied tools for analyzing the effectiveness of external inputs to networked systems is controllability and its related notions such as spectral properties of the controllability Grammian. And, as already noted, controllability is a point-to-point, global property in that it dictates in-between what states it is possible to move the system.

As the setup in this paper is a situation where external inputs (6) are given in conjunction with the secondary objective of ensuring that the agents stay in formation through (8) (e.g., by dragging networked robots toward a target location or in some specified direction). In such situations, a more instantaneous notion of input effectiveness would be useful in that it would capture some local (in time) notion of "progress".

To address the instantaneous effects that the inputs have on the rest of agents, we here introduce the notion of manipulability of leader-follower networks. In fact, we define the manipulability of leader-follower networks based on the ratio between the norm of the followers' velocities and that of the leaders' velocities, similar to the definition used by Bicchi, et al. for robotic manipulators [1,2]. Specifically, we use the following ratio:

$$m(x, \mathsf{E}, \dot{x}_\ell) = \frac{\dot{x}_f^T Q_f \dot{x}_f}{\dot{x}_\ell^T Q_\ell \dot{x}_\ell}, \quad (10)$$

where $Q_f = Q_f^T \succ 0$ and $Q_\ell = Q_\ell^T \succ 0$ are positive definite weight matrices.

Note that the manipulability index is a function of input directions of leaders, network topologies, and agent configurations. Therefore, given such a measure, one of these properties can be optimized when the other two properties are given. As an application of this notion, one can consider the problem of finding the best directions (axes) of inputs, given leader nodes, as the maximization of (10) with respect to $\dot{x}_\ell$ (see also Section 4.2):

$$\dot{x}_{\ell,\max}(x, \mathsf{E}) = \arg \max_{\dot{x}_\ell} \; m(x, \mathsf{E}, \dot{x}_\ell), \quad (11)$$

$$m_{\max}(x, \mathsf{E}) = \max_{\dot{x}_\ell} \; m(x, \mathsf{E}, \dot{x}_\ell). \quad (12)$$

Similarly, the problem of finding the best network topology for given agent configurations and leader inputs can be formulated, for example, by

$$\mathsf{E}_{\max} = \arg \max_{\mathsf{E}} m(x, \mathsf{E}, \dot{x}_\ell) \quad \text{subject to} \quad |\mathsf{E}| \le M_{\lim}, \quad (13)$$

which we will investigate further in Section 5. Another possible application is the selection of effective leaders, which was addressed in [14].

While manipulability is an intuitively clear notion, it needs to be connected to the actual agent dynamics from the previous section in a meaningful way, which presents some difficulty. The reason is that since $\dot{x}_f = -\frac{\partial \mathcal{E}}{\partial x_f}^T$ is a function of x_f and x_ℓ but not $\dot{x}_\ell$, we need to introduce an integral action to see the influence of $\dot{x}_\ell$. However, the input velocity $\dot{x}_\ell$ is not necessarily constant over the time interval of the integration. Thus, it is impossible to calculate an instantaneous measure given by (10).

Two choices present themselves to overcome this difficulty. The first is to change the agent dynamics. But, we do not want to follow that route since edge-tension functions (and weighted consensus equations) are used quite frequently. As such, to define a notion that is practically relevant, we choose to go with a second option instead, namely to introduce an approximate notion of manipulability, i.e., to assume that the followers move fast enough to always maintain the desired distances. Although this is clearly not always the case, we will see in simulation as well as in robotic experiments that it is still a reasonably good approximation of the network dynamics.

4 Approximate Manipulability

As stated, we need to be able to relate the follower velocities to the leader velocities and we achieve this by making the assumption that the inter-agent distances are perfectly maintained between agents that are adjacent in the network. In particular, we assume the connections of agents can be seen as rigid links; once the analogy of kinematic chains is introduced, the rich background of graph rigidity theory [24] and parallel mechanism can be applied to a variety of problems (e.g., see [8] for formation control and [28] for localization of a formation). This section explores how this approximation allows us to produce a well-defined and computable approximate manipulability index.

4.1 Rigid-Link Approximation

We start off by describing what we mean by a rigid-link approximation, which is a concept closely related to rigidity theory:

Definition 4.1 *A rigid-link approximation of the dynamics in (9) is such that all the given desired distances* $\{d_{ij}\}_{\{v_i, v_j\} \in \mathsf{E}}$ *are perfectly maintained by the followers, i.e.,* $\|x_i - x_j\| = d_{ij} \; \forall \{v_i, v_j\} \in \mathsf{E}$.

This approximation [3] makes sense if the scale of the edge-tension energy $\mathcal{E}(t)$, i.e., the control gain of the followers, is large enough compared to that of the leader velocities $\dot{x}_\ell(t)$ in order to achieve an effective time-separation. Note also that, in real situations, $\mathcal{E}(t)$ needs to be greater than zero in order for the followers to move, while this approximation implies $\mathcal{E}(t) = 0 \; \forall t$. Therefore, the situation of Definition 4.1 is never realized perfectly in an actual, practically implemented leader-follower network as long as the leaders are moving. Nevertheless, as will be seen in Section 5, this approximation gives us a good estimation of the actual network responses to injected leader inputs, unless leaders move much faster than followers.

In order to analyze the approximated dynamics, we need to make use of the *rigidity matrix*, e.g., [24,8]. If the connections in agent pairs associated with the edges can be viewed as rigid links, the distances between connected agents do not change in time. Assuming that the trajectories of $x_i(t)$ are smooth and differentiable, then

$$\frac{d}{dt}||x_i - x_j||^2 = 0 \quad \forall \{v_i, v_j\} \in \mathsf{E},$$

and therefore

$$(x_i - x_j)^T (\dot{x}_i - \dot{x}_j) = 0 \quad \forall \{v_i, v_j\} \in \mathsf{E}. \tag{14}$$

Let $R(x) \in \mathbb{R}^{M \times Nd}$ be the rigidity matrix associated to the given state x and the underlying graph G. Then, (14) can be written in the compact form

$$R(x)\dot{x} = 0. \tag{15}$$

Here, each row of the rigidity matrix $R(x)$ consists of N blocks of d-dimensional row vectors. In the k-th row ($k = 1, ..., M$), its i_k-th and j_k-th blocks are $(x_{i_k} - x_{j_k})^T$ and $-(x_{i_k} - x_{j_k})^T$, respectively (the signs of these two blocks can be swapped), and other blocks are zeros, where i_k and j_k are the agents connected by edge k.

Substituting the time derivative of (2) into (15) yields

$$R_f(x)\dot{x}_f + R_\ell(x)\dot{x}_\ell = 0, \tag{16}$$

where $R_f \in \mathbb{R}^{M \times N_f d}$ and $R_\ell \in \mathbb{R}^{M \times N_\ell d}$ are defined by

$$R_\ell(x) \triangleq R(x)(\Delta_\ell \otimes I_d), \;\; R_f(x) \triangleq R(x)(\Delta_f \otimes I_d). \tag{17}$$

Assume that the leaders move in a feasible manner so that the approximation in Definition 4.1 remains appropriate. From the constraint equation (16), the possible

set of $\dot{x}_f$ associated with $\dot{x}_\ell$ can be obtained as the general solution:

$$\dot{x}_f = -R_f^\dagger R_\ell \dot{x}_\ell + [\text{null}(R_f)]p, \tag{18}$$

where $R_f^\dagger$ is the Moore-Penrose pseudo inverse of R_f, $[\text{null}(R_f)]$ is a matrix whose columns span $\text{null}(R_f)$, and $p \in \mathbb{R}^{\text{nullity}(R_f)}$ is arbitrary, where $\text{nullity}(R_f) = \dim(\text{null}(R_f)) = N_f d - \text{rank}(R_f)$. That is, infinite possibilities of $\dot{x}_f$ may exist once the input $\dot{x}_\ell$ is given. For instance, if $N_\ell = 1$, then $\text{nullity}(R_f) \geq d(d-1)/2$, which means that at least the rotational degrees of freedom around the leader always remain.

In indeterminate cases, the value of the manipulability index (10) cannot be determined uniquely, and it seems that we need to modify the definition of manipulability, for example, by using the "worst-case approach" [2] that assumes the least end-effector velocity (follower velocity, in our case). However, once we consider the follower dynamics (8) in the rigid-link approximation (Definition 4.1), we will see that $p = 0$ is a reasonable choice in (18) to determine the followers' response to the leaders' movement. This is the key for introducing the notion of manipulability in leader-follower networks with an approximated dynamics. In the following paragraphs, we prepare some facts and then show how $\dot{x}_f$ is indeed determined uniquely.

Lemma 4.1 *Let $A \in \mathbb{R}^{n \times n}$ be a negative semidefinite matrix, which can be decomposed into $A = -V\Lambda V^T \preceq 0$, where the i-th column vector of $V \in \mathbb{R}^{n \times r}$ is an eigenvector corresponding to eigenvalue $\lambda_i > 0 \quad (i = 1, ..., r)$, $r = \text{rank}(A)$, $\Lambda = \text{Diag}([\lambda_1, ..., \lambda_r])$, and $V^T V = I_r$. Then, the following holds:*

$$\left(\lim_{t \to \infty} \int_0^t e^{A(t-\tau)} d\tau\right) V = V\Lambda^{-1}. \tag{19}$$

PROOF. Using the fact that $e^{-V\Lambda V^T t} - I_n = \sum_{k=1}^\infty \frac{t^k}{k!} V(-\Lambda)^k V^T = V(e^{-\Lambda t} - I_r)V^T$ with $V^T V = I_r$,

$$L.H.S. = \lim_{t \to \infty} \int_0^t \left(V(e^{-\Lambda(t-\tau)} - I_r) + V\right) d\tau$$

$$= V \lim_{t \to \infty} \int_0^t e^{-\Lambda(t-\tau)} d\tau$$

$$= V \lim_{t \to \infty} \text{Diag}\left(\left[\frac{1 - e^{-\lambda_1 t}}{\lambda_1}, \cdots, \frac{1 - e^{-\lambda_r t}}{\lambda_r}\right]\right)$$

$$= R.H.S. \quad \square$$

Lemma 4.2 *Given a linear system $\dot{x}(t) = Ax(t) + Bu$ with $x(0) = 0$ and constant input $u \in \mathbb{R}^b$, where $A \in \mathbb{R}^{n \times n}$ and $B \in \mathbb{R}^{n \times b}$ are time-invariant matrices that can be decomposed into $A = -G^T G$ and $B = G^T H$, respectively, where $G \in \mathbb{R}^{a \times n}$, $H \in \mathbb{R}^{a \times b}$, and $a \in \mathbb{N}$, the state converges to $\lim_{t \to \infty} x(t) = G^\dagger H u$.*

---

[3] This should be distinguished from rigid formations, referred to as "rigid frameworks", e.g., [24]. Flexible (non-rigid) formations can be considered under the rigid-link approximation.

PROOF. Let $G = U\Sigma V^T$ be the singular value decomposition of G, where $U \in \mathbb{R}^{a \times r}$ and $V \in \mathbb{R}^{n \times r}$ are column-orthogonal matrices (i.e., $V^T V = I_r$ and $U^T U = I_r$), $\Sigma \in \mathbb{R}^{r \times r}$ is a diagonal matrix, and $r = \text{rank}(A) \le \min\{n, a\}$. Then, the zero-state response of the system converges to

$$
\begin{aligned}
\lim_{t \to \infty} x(t) &= \lim_{t \to \infty} \int_0^t e^{A(t-\tau)} d\tau B u \\
&= \left(\lim_{t \to \infty} \int_0^t e^{-V \Sigma^2 V^T (t-\tau)} d\tau V \right) \Sigma U^T H u \\
&= (V \Sigma^{-2}) \Sigma U^T H u = (V \Sigma^{-1} U^T) H u,
\end{aligned}
$$

where we used Lemma 4.1. Note that all the diagonal elements in Σ are non-zero (strictly positive); hence, Σ^{-1} exists and $G^\dagger = V \Sigma^{-1} U^T$. $\square$

Lemma 4.3 *The second-order partial derivatives of the edge-tension energy (3) with respect to x_f and x_ℓ have the following form when all the connected agents satisfy their desired distances at $x = x^*$ (i.e., $||x_i - x_j|| = d_{ij} \ \forall \{v_i, v_j\} \in \mathsf{E}$):*

$$
\left. \frac{\partial^2 \mathcal{E}}{\partial x_f^2} \right|_{x=x^*} = S_f^T S_f, \qquad \left. \frac{\partial^2 \mathcal{E}}{\partial x_f \partial x_\ell} \right|_{x=x^*} = S_f^T S_\ell,
$$

where $\frac{\partial^2 \mathcal{E}}{\partial x_f^2} \in \mathbb{R}^{N_f d \times N_f d}$, $\frac{\partial^2 \mathcal{E}}{\partial x_f \partial x_\ell} \in \mathbb{R}^{N_f d \times N_\ell d}$, and

$$
S_f = W' R_f, \quad S_\ell = W' R_\ell.
$$

Here, $W' \in \mathbb{R}^{M \times M}$ is a diagonal matrix whose elements are

$$
[W']_{kk} = \left(\frac{w'_{i_k j_k}(d_{i_k j_k})}{d_{i_k j_k}} \right)^{\frac{1}{2}} = \frac{e'_{i_k j_k}(d_{i_k j_k})}{d_{i_k j_k}} \quad (k = 1, ..., M),
$$

where, i_k and j_k are the two agents connected by edge k, and where $w'_{ij}(z) \triangleq \frac{dw_{ij}(z)}{dz}$.

PROOF. See appendix A. $\square$

Recall that we assumed $d_{ij} \in (0, \infty)$ and that $e_{ij}(z)$ is a strictly increasing, twice differentiable function for all $\{v_i, v_j\} \in \mathsf{E}$. Therefore, $[W]_{kk} \in (0, \infty)$ always exists for all $k \in \{1, ..., M\}$.

Example 4.1 *If the edge-tension energy is given by (5), then $e'_{ij}(z) = c_{ij}$ and $[W']_{kk} = c_{i_k j_k}/d_{i_k j_k}$ ($k = 1, ..., M$).*

In what follows, we assume single-leader networks and that the leader can move arbitrarily, while the result here can be extended to multi-leader cases [13].

Lemma 4.4 *If $N_\ell = 1$, then $R_f^\dagger R_\ell = S_f^\dagger S_\ell$.*

PROOF. Since all diagonal elements in W' are non-zero, R_f and $S_f = W' R_f$ have the same row space. Therefore, their projection matrices onto the row space are identical:

$$
R_f^\dagger R_f = S_f^\dagger S_f. \tag{20}
$$

Now, since we assume that $N_\ell = 1$, the matrices R_f and S_f have the following properties, respectively:

$$
R_f(\mathbf{1}_{N_f} \otimes I_d) = -R_\ell, \quad S_f(\mathbf{1}_{N_f} \otimes I_d) = -S_\ell. \tag{21}
$$

In other words, a state-component-wise summation in each row of R_f is equal to the corresponding element in the same row of $-R_\ell$ (due to the definition of the rigidity matrix R); i.e., $\sum_{i=1}^{N_f} [R_f]_{k,((i-1)d+j)} = -[R_\ell]_{k,j} \quad \forall j \in \{1, ..., d\}, \forall k \in \{1, ..., M\}$. Therefore, using (21) with (20), we obtain $R_f^\dagger R_\ell = -R_f^\dagger R_f(\mathbf{1}_{N_f} \otimes I_d) = -S_f^\dagger S_f(\mathbf{1}_{N_f} \otimes I_d) = S_f^\dagger S_\ell$. $\square$

Theorem 4.1 *If $N_\ell = 1$ (i.e., single-leader case), the rigid-link approximation of dynamics (8) is given by*

$$
\dot{x}_f(t) = -R_f^\dagger R_\ell \dot{x}_\ell(t). \tag{22}
$$

PROOF. We here define the approximation described in Definition 4.1 in a more formal way. Consider that the velocity of leaders gives a small displacement, $\delta x_\ell(t)$, of their state from time t to $t + \delta t$. Here, $\dot{x}_\ell(t) = \lim_{\delta t \to 0} \frac{\delta x_\ell(t)}{\delta t}$. Since we assume that the desired distances are perfectly maintained by the followers, we introduce another time axis s and track the state of followers, $\tilde{x}_f(t, s) \triangleq x_f(t) + \delta \tilde{x}_f(t, s)$, to see its convergence in $s \to \infty$, where the leader's state $\tilde{x}_\ell(t, s) \triangleq x_\ell(t) + \delta x_\ell(t)$ is constant on the axis of s. We can think of s describing the time evolution when the system is executing the actual, as opposed to the approximate, dynamics. Then, we consider the approximation in Definition 4.1 as $\dot{x}_f(t) = \lim_{\delta t \to 0} \lim_{s \to \infty} \frac{\delta \tilde{x}_f(t, s)}{\delta t}$. We also assume that $\tilde{x}_f(t, 0) = x_f(t)$ and that all the desired distances are satisfied at $s = 0$.

Since the actual dynamics of the followers is given by (8), the system equation of $\delta \tilde{x}_f(t, s)$ becomes

$$
\begin{aligned}
\frac{d}{ds} \delta \tilde{x}_f(t, s) &= \frac{d}{ds} \tilde{x}_f(t, s) = -\frac{\partial \mathcal{E}(\tilde{x}_f(t, s), \tilde{x}_\ell(t, s))}{\partial x_f}^T \\
&= -\frac{\partial \mathcal{E}(x_f(t) + \delta \tilde{x}_f(t, s), x_\ell(t) + \delta x_\ell(t))}{\partial x_f}^T \\
&= -\frac{\partial^2 \mathcal{E}(x_f(t), x_\ell(t))}{\partial x_f^2} \delta \tilde{x}_f(t, s) - \frac{\partial^2 \mathcal{E}(x_f(t), x_\ell(t))}{\partial x_f \partial x_\ell} \delta x_\ell(t),
\end{aligned}
$$

where we assumed that $\delta x_\ell(t)$ and $\delta \tilde{x}_f(t, s)$ are small enough to use the first-order approximation. We also used $\frac{\partial \mathcal{E}(x_f(t), x_\ell(t))}{\partial x_f} = 0$. Note that $\frac{\partial^2 \mathcal{E}(x_f(t), x_\ell(t))}{\partial x_f^2}$ and $\frac{\partial^2 \mathcal{E}(x_f(t), x_\ell(t))}{\partial x_f \partial x_\ell}$ are constant on the time axis of s.

Using Lemma 4.3, we can rewrite the above system as

$$\frac{d}{ds}\delta\tilde{x}_f(t,s) = -(S_f^T S_f)\delta\tilde{x}_f(t,s) - (S_f^T S_\ell)\delta x_\ell(t). \quad (23)$$

Recall that the initial condition is $\delta\tilde{x}_f(t,0) = 0$ and $\delta x_\ell(t)$ is constant on the axis s. Therefore, using Lemma 4.2, we know that (23) converges and its convergence point is given by

$$\delta x_f(t) \triangleq \lim_{s\to\infty}\delta\tilde{x}_f(t,s) = -S_f^\dagger S_\ell \delta x_\ell(t). \quad (24)$$

Here, $\delta x_f(t)$ gives the displacement of the followers caused by the displacement $\delta x_\ell(t)$. Thus, dividing (24) by δt and taking $\delta t \to 0$, we obtain

$$\dot{x}_f(t) = -S_f^\dagger S_\ell \dot{x}_\ell(t). \quad (25)$$

Finally, if $N_\ell = 1$, (25) and Lemma 4.4 yield (22). $\quad\square$

Regarding $N_\ell > 1$ cases, it can be shown that (22) also holds if the motion of leaders is constrained not to violate the rigid-link approximation (see [13] for details). Note also that (22) does not depend on a specific choice of function e_{ij} in (4).

4.2 Manipulability with the Rigid-Link Approximation

As a corollary to Theorem 4.1, the manipulability (10) of leader-follower networks under the rigid-link approximation of the follower dynamics is given by the Rayleigh quotient

$$\hat{m}(x, \mathsf{E}, \dot{x}_\ell) = \frac{\dot{x}_\ell^T J^T Q_f J \dot{x}_\ell}{\dot{x}_\ell^T Q_\ell \dot{x}_\ell}, \quad (26)$$

which we refer to as the *approximate manipulability*, where $J(x, \mathsf{E}) \triangleq -R_f^\dagger R_\ell$. Hence, similar to the manipulability indices in robot-arm manipulators, the maximum/minimum values of the manipulability index can be obtained through spectral analysis. That is, $\hat{m}_{\max}(\triangleq \max_{x_\ell}\hat{m})$ is the maximum eigenvalue $\lambda_{\max}$ of the generalized eigenvalue problem $J^T Q_f J v = \lambda Q_\ell v$, and $\dot{x}_{\ell,\max}(\triangleq \arg\max_{x_\ell}\hat{m})$ is obtained from its corresponding eigenvector $v_{\max}$ as $\dot{x}_{\ell,\max} = \alpha v_{\max}$ $(\alpha \neq 0)$. Similarly, $\hat{m}_{\min}(\triangleq \min_{x_\ell}\hat{m})$ and its corresponding inputs are obtained as the minimum eigenvalue $\lambda_{\min}$ and from its corresponding eigenvector, respectively.

Note that this analysis determines only an effective "axis" of inputs. To find an effective direction including the sign of α, additional analysis on the temporal change of $\hat{m}_{\max}$ will be required.

The following proposition shows the range of $\hat{m}$ under a typical choice of N_ℓ, Q_f, and Q_ℓ.

Proposition 4.1 *Suppose $N_\ell = 1$, $Q_f = I_{N_f d}$, and $Q_\ell = I_d$. The approximate manipulability $\hat{m}$ takes*

$$0 \le \hat{m} \le N_f.$$

PROOF. Since $J^T J \succeq 0$, $0 \le \lambda_{\min}(J^T J) \le \hat{m} \le \lambda_{\max}(J^T J)$ holds. Meanwhile, $\lambda_{\max}(J^T J) = \lambda_{\max}((\mathbf{1}_{N_f}^T \otimes I_d)(R_f^\dagger R_f)^2 (\mathbf{1}_{N_f} \otimes I_d)) \le \lambda_{\max}((\mathbf{1}_{N_f}^T \otimes I_d)(\mathbf{1}_{N_f} \otimes I_d)) = \lambda_{\max}(N_f I_d) = N_f$ since $R_f^\dagger R_f$ is a projection matrix. Hence, the proposition follows. $\quad\square$

It should be pointed out that the approximate manipulability can also be interpreted in terms of the measure of how much the motion of the followers' centroid coincides with the leader's motion:

Proposition 4.2 *Suppose $N_\ell = 1$ and $Q_f = I_{N_f d}$. Let $\bar{x}_f = \frac{1}{N_f}(\mathbf{1}_{N_f}^T \otimes I_d)x_f$ be the centroid of the follower agents. Then, we have $\frac{1}{N_f}\hat{m} = \dot{x}_\ell^T \dot{\bar{x}}_f/(\dot{x}_\ell^T Q_\ell \dot{x}_\ell)$.*

PROOF. Using the fact that $(R_f^\dagger R_f)^2 = R_f^\dagger R_f$, we have $J^T J = (\mathbf{1}_{N_f}^T \otimes I_d)(R_f^\dagger R_f)(\mathbf{1}_{N_f} \otimes I_d) = (\mathbf{1}_{N_f}^T \otimes I_d)J$. Hence, $\dot{x}_\ell^T J^T J \dot{x}_\ell = \dot{x}_\ell^T (\mathbf{1}_{N_f}^T \otimes I_d)J\dot{x}_\ell = \dot{x}_\ell^T (\mathbf{1}_{N_f}^T \otimes I_d)\dot{x}_f = N_f \dot{x}_\ell^T \dot{\bar{x}}_f$, and the proposition follows. $\quad\square$

4.3 Leader-Side Manipulability Ellipsoids

Now, we introduce a tool to depict effective input directions (axes) in the case of $Q_\ell \propto I_{N_\ell d}$. Let us first consider a robot-arm manipulability index defined by $\frac{\dot{r}^T \dot{r}}{\dot{\theta}^T \dot{\theta}}$, where θ and r are the states of joint angles and the end-effector, respectively. Given a kinematic relation $r = f(\theta)$, the relation between $\dot{r}$ and $\dot{\theta}$ becomes $\dot{r} = \frac{\partial f}{\partial \theta}\dot{\theta}$. Then, by using Jacobian $\frac{\partial f}{\partial \theta}$, the manipulability ellipsoid [27] can be defined as $\dot{r}^T(\frac{\partial f}{\partial \theta}\frac{\partial f}{\partial \theta}^T)^\dagger \dot{r} = 1$, which depicts the range of end-effector velocities under a given input $\dot{\theta}$ with norm $||\dot{\theta}|| \le 1$.

In contrast, since our interest is in the effective direction (axis) of inputs, we define a similar ellipsoid not in the space of follower velocities but in the space of leader velocities (see Fig. 2 for example):

$$\dot{x}_\ell^T (J^T Q_f J)^\dagger \dot{x}_\ell = \text{const.}, \quad (27)$$

which we refer to as the *leader-side manipulability ellipsoid*. Here, the longest axis of the ellipsoid is given by the eigenvector that corresponds to the maximum eigenvalue of $J^T Q_f J$.
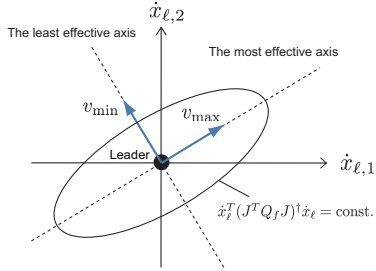
Fig. 2. Leader-side ellipsoid in the input space ($N_\ell = 1, d = 2$ case). The most effective axis is given by the eigenvector $v_{\max}$ that corresponds to the maximum eigenvalue $\lambda_{\max}(J^T Q_f J)$.

5 Examples

In the following examples, we first verify the approximation of dynamics, and we then show how the defined manipulability index can be used to analyze effectiveness of leader inputs in simulation and with mobile robots. Finally, we demonstrate the optimization of network topologies. For simplicity, we consider single-leader networks in $\mathbb{R}^2$ (i.e., $d = 2$), and we use $Q_f = I_{2N_f}$ and $Q_\ell = I_{2N_\ell}$ for the weight matrices in (10). Note that, here, x_i corresponds to agent i's two dimensional position, and state x denotes a positional configuration of the constituent agents.

5.1 Rigid-Link Approximation

In order to examine the approximation of the follower dynamics shown in Theorem 4.1, we compared follower trajectories generated by the original dynamics (8) and the rigid-link approximated dynamics (22). The function in (5) with uniform weights $c_{ij} = c$ was used for the edge-tension energy of the follower dynamics (8), and $\dot{x}_\ell(t) = [0, \alpha]^T$ (α : const.) was used for the leader's velocity. All the desired distances, d_{ij} $\forall \{v_i, v_j\} \in E$, were set to be 1. Since the scale of the control gain of followers is dictated by c^2 in (4) and (5), the validity of the rigid-link approximation is determined by a parameter pair (α, c); for example, if α is small and c is large enough, the followers almost maintain the desired distances. Meanwhile, as shown in Fig. 3, the distances between connected agents vary more when smaller c is given.

To verify this characteristics, 500 feasible formations with $N = 7$ were generated randomly: Starting from a node, each formation was generated by iteratively adding a link (a new node and an edge with a random angle to an existing node) and a triangle (a new node and two edges to an existing edge). A randomly chosen node was assigned as a leader in each formation. Then, for each of 18 different pairs of (α, c), the errors between the follower trajectories were calculated and averaged over the formations (Fig. 4). Here, in each trial with a formation and a parameter set (α, c), the error was measured by $E(\alpha, c) = \frac{1}{T_\alpha N_f} \int_0^{T_\alpha} \|x_f^{(o)}(t; \alpha, c) - x_f^{(a)}(t; \alpha)\| dt$,
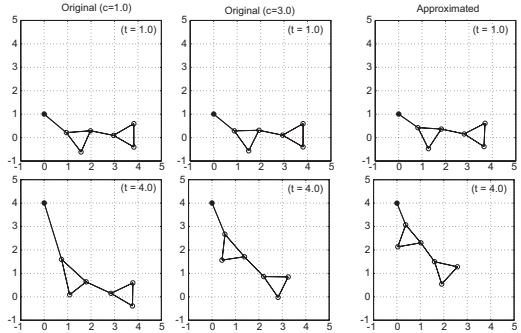

Fig. 3. Example of the original dynamics (left, middle), given by (8) with $c = 1, 3$, and the approximated dynamics (right), given by (22). $\alpha = 1$ was used for the leader's velocity.
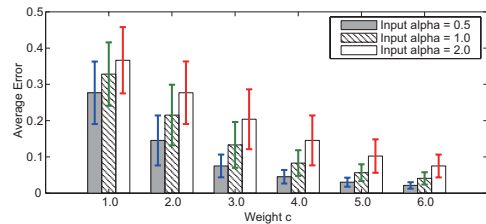

Fig. 4. Average error between original and approximated follower trajectories (error bars represent the standard deviations). For each pair (α, c), the trajectory errors were averaged over randomly generated 500 formations .

where $x_f^{(o)}(t; \alpha, c)$ and $x_i^{(a)}(t; \alpha)$ are trajectories generated by the original and the approximated dynamics, respectively, where $T_\alpha = 5/\alpha$ (i.e., the leader finally moved $[0, 5]^T$ in every trial).

We observe that large c and small α achieve smaller error. However, in real situations with communication/sensing time delays, high gains of followers may cause instability. For example, in the formation in Fig. 3, chattering has occurred when the delay exceeded around $0.45, 0.04, 0.01$ for $c = 1, 3, 5$ (with any $\alpha \in \{0.5, 1.0, 2.0\}$), respectively, where we assumed a uniform delay for all agent pairs. Hence, given large time delays, smaller α should be used to obtain small approximation errors. Nevertheless, the leader's velocity in real applications has a certain appropriate range, and an approximation error therefore always exists. In Section 5.3, we will examine and interpret the gap of approximation using actual mobile robots.

5.2 Approximate Manipulability

To see how the proposed index can capture the effectiveness of leader inputs depending on agent configurations, we first used a line graph with $N_f = 6$ and $N_\ell = 1$, and compared two motions started from the same initial configuration shown in Fig. 5 (a). The leader's inputs were given by constant velocities, $\dot{x}_\ell = [\cos(\theta), \sin(\theta)]^T$ with $\theta = 0$ and $\theta = \pi$, and the approximated follower dynamics (22) were used here to focus on examining the index properties in ideal situations. The intermediate configu-

8

(a) Initial agent configuration ($t = 0$)

(b) $t = 2$ (with $\theta = \pi$)

(c) $t = 2$ (with $\theta = 0$)

(d) Temporal change of $\hat{m}$ during two motions
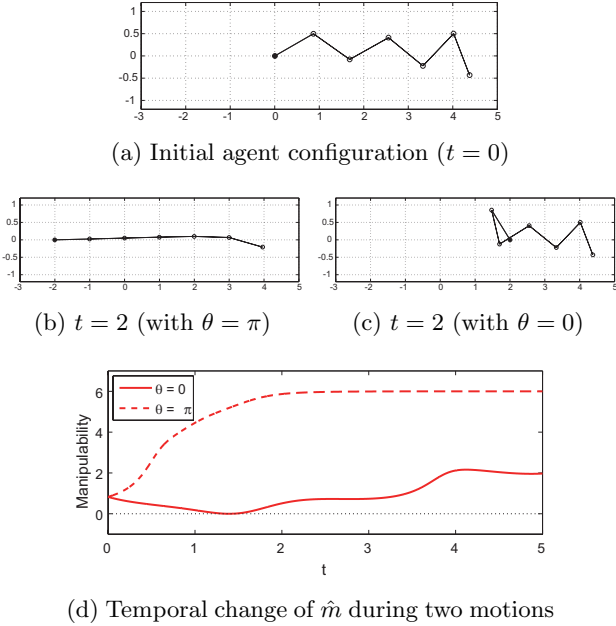
Fig. 5. Comparison of the temporal change of the approximate manipulability $\hat{m}$ when the leader moves toward two opposite directions: $\theta = 0$ and π.

ration at $t = 2$ are shown in Fig. 5 (b) and Fig. 5 (c).

Fig. 5 (d) shows the temporal change of the approximate manipulability $\hat{m}$ in each of the two motions. When the leader moved toward right with $\theta = 0$, the value of $\hat{m}$ changed between around 0 and 2; meanwhile, when the leader moved with $\theta = \pi$, which stretched the network, $\hat{m}$ increased monotonically and it converged almost 6, which is the maximum value of $\hat{m}$ in this setting according to Proposition 4.1. That is, in terms of the followers' response to the leader's injected input into this network, the leader motion dragging the entire network is more effective than the motion moving toward the centroid of the agents. This fact can also be predicted by Proposition 4.2 as all the directions of the leader and the followers coincide if the network is in a straight-line formation.

As an example to see the change of the leader-side manipulability ellipsoid depending on configurations, we used the graph with $N = 3$ ($N_f = 2$ and $N_\ell = 1$) and $|\mathsf{E}| = 2$, where the leader moved with $\dot{x}_\ell(t) = [1, 0]^T$. From the ellipsoids depicted in Fig. 6 (a), we see that the horizontal direction was effective in the first and last parts of the motion, while the vertical direction was effective in the middle (around $t = 1$).

5.3 Experiment with Mobile Robots

We conducted an experiment with mobile robots (Khepera III, K-TEAM) to see the characteristics of the manipulability index in real situations. Although our focus in this paper is on single-integrator models, we here ex-
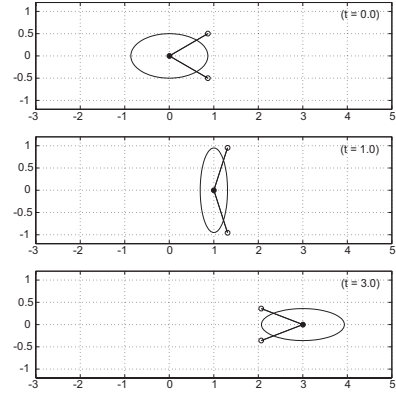

Fig. 6. Leader-side manipulability ellipsoids.

amined mobile robots with kinematics in order to discuss possible extensions of the proposed index.

Each of the robots has two wheels and therefore its kinematics need to be considered. Let $x_i \in \mathbb{R}^2$ be the center of robot (agent) i, and let $\dot{x}_i = u_i \in \mathbb{R}^2$ be the control input to the robot i. First, we approximate the kinematics of each robot as the unicycle model:

$$\dot{x}_i = v_i r_1(\theta_i), \qquad \dot{\theta}_i = \omega_i, \qquad (28)$$

where $r_1(\theta_i) = [\cos(\theta_i), \sin(\theta_i)]^T$. To obtain the linear velocity v_i and angular velocity ω_i from the control input u_i, we consider the near-identity diffeomorphism [22]. In particular, we control the off-centered point

$$x'_i = x_i + \varepsilon r_1(\theta_i) \qquad (29)$$

with a small enough constant ε; that is, we use $\dot{x}'_i = u_i$ instead of $\dot{x}_i = u_i$. Substituting (28) into the time derivative of (29) yields [4]

$$v_i = r_1(\theta_i)^T u_i, \quad \omega_i = (1/\varepsilon) r_2(\theta_i)^T u_i,$$

where $r_2(\theta_i) = [-\sin(\theta_i), \cos(\theta_i)]^T$. Finally, the speeds of left and right wheels are obtained as $v_{l,i} = v_i - (d_w/2)\omega_i$ and $v_{r,i} = v_i + (d_w/2)\omega_i$, respectively, where d_w is the distance between the two wheels.

As shown in Fig. 7, three robots were used for this experiment, where one was assigned as a leader ($i = 3$) and the remaining two were assigned as followers ($i = 1, 2$). A motion capture system (VICON) was used to obtain the position of each robot. [5] The scenario (i.e., initial positions, topology, and the leader's motion) was similar to the last example (Fig. 6). Regarding leader's input $u_\ell = u_3$, the leader robot moved toward one direction from

---

[4] Each follower does not need θ_i in the implementation, since the control input can be given in each local coordinate.

[5] While a decentralized control can be achieved with the robots' local sensors, we used a motion capture system, which is considered to be more reliable than the local sensors, since our focus is to examine the features of the proposed index.

(a) t=0   (b) t=3.3   (c) t=6.7   (d) t=10   (e) t=13.3

(f) t=16.7   (g) t=20   (h) t=23.3   (i) t=26.7   (j) t=30
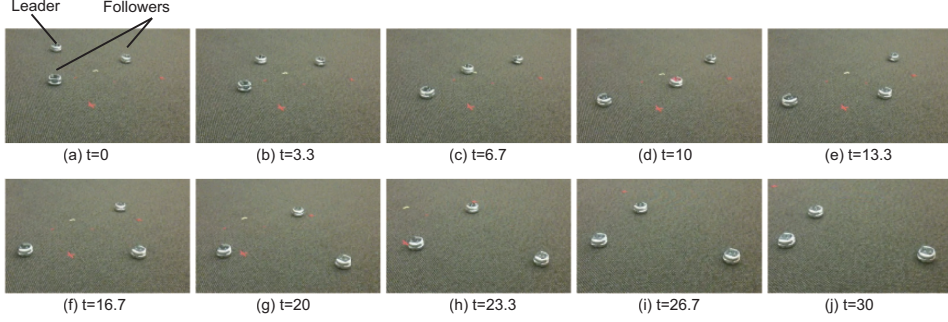
Fig. 7. The motion of mobile robots during the experiments: A leader robot starts to move toward the center between two follower robots (a). The follower robots are changing their headings and moving toward outside to maintain the desired distances from the leader ((b) to (d)). Once the leader passed between the followers, the followers change their headings again ((e) to (f)) and follow the leader to keep the desired distances ((g) to (j)).
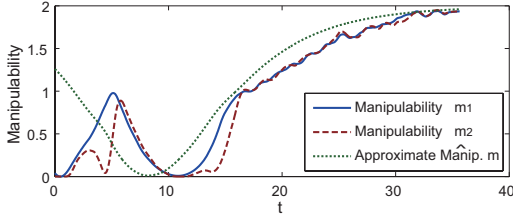

Fig. 8. Comparison of the manipulability indices. Two indices, m_1 and m_2, are used for the original manipulability to see the effects of the approximation of individual kinematics.

the initial position with a constant velocity (9.5cm/s) as shown in Fig. 7. The desired distance between the leader and each of the followers was set to 80cm, and was almost satisfied in the initial positions. The parameter ε in (29) was chosen to be $\varepsilon = d_w/2$, where $d_w = 8.85$cm. The weight in (5) was set to $c_{ij} = 0.6$ for both edges by taking into account the scale of the relative positions and the maximum speed of the robots.

Fig. 8 shows the comparison of the following three indices during the scenario of Fig. 7:

$$m_1 = \frac{u_f^T u_f}{\dot{x}_\ell^T \dot{x}_\ell}, \quad m_2 = \frac{\dot{x}_f^T \dot{x}_f}{\dot{x}_\ell^T \dot{x}_\ell}, \quad \hat{m} = \frac{\dot{x}_\ell J(x)^T J(x) \dot{x}_\ell}{\dot{x}_\ell^T \dot{x}_\ell},$$

where $x(t) = [x_f(t)^T, x_\ell(t)^T]^T$ with $x_f = [x_1^T, x_2^T]^T$ and $x_\ell = x_3$ is the measured positions of the robots, and $u_f(t) = [u_1(t)^T, u_2(t)^T]^T = -\frac{\partial \mathcal{E}(x)}{\partial x_f}^T$ is the control input to the followers. We here used two indices, m_1 and m_2, for the original manipulability since $\dot{x}_i = u_i$ is not perfectly satisfied for each robot due to (28) and (29).

As is the case in Fig. 6, the index $\hat{m}$ once had a small value in the middle (around $t = 10$) because the robots lined perpendicular to the moving direction of the leader. The difference between m_1 (solid) and $\hat{m}$ (dotted) is due to the rigid-link approximation. Note that this difference can be considered as a preferable property of the index $\hat{m}$ rather than the approximation error. That is, in the rigid-link approximation (Definition 4.1), we assume the

convergence of the followers in every time point. Therefore, the approximate manipulability $\hat{m}$ essentially performs a short-term prediction of the input influence. In fact, $\hat{m}$ at $t = 0$ had a large value because of the predicted effect of the leader's input while the original manipulability m_1 was almost zero.

On the other hand, the difference between m_1 (solid) and m_2 (dashed) was mainly caused by the approximation with (28) and (29). In particular, the major discrepancies around $t = 4$ and around $t = 15$ are due to the kinematics of the unicycle model (28), since the followers were changing their heading directions significantly in these periods. While this paper assumes single-integrator models in the theoretical contributions, the extension of the approximate manipulability to a variety of robot/agent models should be addressed in future.

5.4 Optimization of Network Topologies

To demonstrate how the notion of manipulability can be used to find effective topologies, we first compared the values of the approximate manipulability in different topologies with different input directions. In fact, we considered four formations, $F_i = (x, \mathsf{G}_i)$ $(i = 1, ..., 4)$, shown in Fig. 9, where the agent configurations, x, were identical. Two input directions $\dot{x}_\ell = [\epsilon, \epsilon]^T$ and $\dot{x}_\ell = [\epsilon, -\epsilon]^T$ were used. Here, $\epsilon > 0$ can be arbitrary since the scale of inputs is normalized in the index $\hat{m}$. Table 1 shows the values of approximate manipulability $\hat{m}$ for each formation and input direction.

For the leader's motion $\dot{x}_\ell = [\epsilon, \epsilon]^T$, the values of index $\hat{m}$ in formation F_3 and F_4 took almost the maximum, according to Proposition 4.1. Formation F_1 also provided a relatively high value despite of the smaller number of edges ($|\mathsf{E}| = 3$). This indicates that the existence of the diagonal edge from the leader was crucial to pull the bottom-left agent toward the upper-right direction. In the case $\dot{x}_\ell = [\epsilon, -\epsilon]^T$, on the other hand, no formation took a prominent value. This is because the

10

(a) F_1 (b) F_2 (c) F_3 (d) F_4
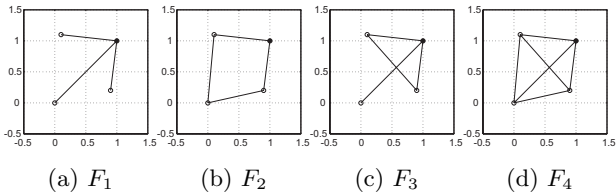
Fig. 9. Formations with $N = 4$ (filled circle: leader).

Table 1
Comparison of the manipulability in different topologies.

Formation	$|\mathsf{E}|$	$\hat{m}$ ($\dot{x}_\ell = [\epsilon, \epsilon]^T$)	$\hat{m}$ ($\dot{x}_\ell = [\epsilon, -\epsilon]^T$)
F_1	3	2.0133	0.9867
F_2	4	1.0522	1.0094
F_3	4	2.9694	1.0170
F_4	5	2.9870	1.0274

leader caused, roughly, a rotating motion of the network around the bottom-left node. Therefore, the edges connecting the leader and other two nodes had a large effect, which were shared by all the four formations.

We then optimized the topologies using the approximate manipulability index given the maximum number of edges (i.e., a limitted communication capacity). Since our focus is on how the proposed index can be applied to find effective network topologies, we used the brute-force search with $N = 5$ and $N = 6$ to find the global optimum instead of using an approximate search algorithm. The given agent configurations are shown in Fig. 10 (left). Two input directions were given to find the optimal topology in Fig. 10 (middle). As for the optimization problem, we solved (13) by using $\hat{m}$ instead of the original manipulability m, where we used $M_{\lim} = N$ for the upper limit of the number of edges.

The effectiveness of the optimized topology was demonstrated by the short-term response of the network in Fig. 10 (right). We see that the topologies were selected appropriately to enhance the effect of given inputs. Future work includes finding an effective, adaptive graph process and algorithms for selecting optimal network topologies when given inputs change continuously.

6 Conclusions

In this paper, we introduced the notion of manipulability in leader-follower networks in order to measure the instantaneous influence of leaders' inputs to followers' response in terms of how inputs through the leaders have impacts on the response of followers. The rigid-link approximation of the network dynamics enables us to find the instantaneous relation between the velocities of leaders and followers, which is crucial to define the approximate manipulability index in a form of the Rayleigh quotient. We have shown, in simulation and with real mobile
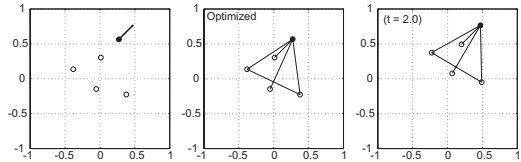

(a) $N = 5$, $\dot{x}_\ell = (0.1, 0.1)^T$, $\hat{m} = 4.861$
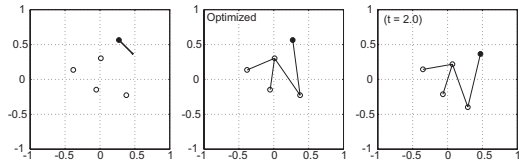
(b) $N = 5$, $\dot{x}_\ell = (0.1, -0.1)^T$, $\hat{m} = 1.657$
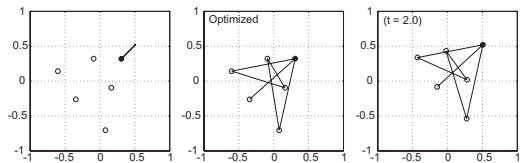
(c) $N = 6$, $\dot{x}_\ell = (0.1, 0.1)^T$, $\hat{m} = 3.693$
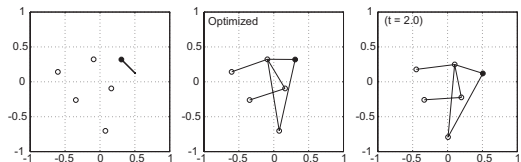
(d) $N = 6$, $\dot{x}_\ell = (0.1, -0.1)^T$, $\hat{m} = 1.220$

Fig. 10. Given agent positions and input directions (left), optimized topology (middle), and the short-term response of the network (right), where $c = 3$ was used to see the response.

robots, that the proposed index successfully captures the effectiveness of leader inputs depending on agent configurations, network topologies, and directions of inputs to the network, and demonstrated an application to find effective network topologies.

Acknowledgments

References

[1] A. Bicchi, C. Melchiorri, and D. Balluchi. On the mobility and manipulability of general multiple limb robots. *IEEE Trans. on Robotics and Automation*, 11(2):215–228, 1995.

[2] A. Bicchi and D. Prattichizzo. Manipulability of cooperating robots with unactuated joints and closed-chain mechanisms. *IEEE Trans. on Robotics and Automation*, 16(4):336–345, 2000.

[3] F. Bullo, J. Cortes, and S. Martinez. *Distributed Control of Robotic Networks*. Princeton University Press, 2009.

[4] Y. Cao and W. Ren. Containment control with multiple stationary or dynamic leaders under a directed interaction graph. *IEEE Conf. on Decision and Control*, pages 3014–3019, 2009.

[5] M. L. Cummings. Human supervisory control of swarming networks. *2nd Annual Swarming: Autonomous Intelligent Networked Systems Conference*, 2004.

[6] J.-P. de la Croix and M. Egerstedt. Controllability characterizations of leader-based swarm interactions. *AAAI Symposium on Human Control of Bio-Inspired Swarms*, 2012.

[7] J. P. Desai, J. P. Ostrowski, and V. Kumar. Modeling and control of formations of nonholonomic mobile robots. *IEEE Trans. on Robotics and Automation*, 17(6):905–908, 2001.

[8] T. Eren and P. N. Belhumeur. A framework for maintaining formations based on rigidity. *Proc. 15th IFAC World Congress*, pages 2752–2757, 2002.

[9] J. A. Fax and R. M. Murray. Graph Laplacians and stabilization of vehicle formations. *Proc. 15th IFAC World Congress*, pages 283–288, 2002.

[10] G. Ferrari-Trecate, M. Egerstedt, A. Buffa, and M. Ji. Laplacian sheep: A hybrid, stop-go policy for leader-based containment control. *Hybrid Systems: Computation and Control*, pages 212–226, 2006.

[11] A. Jadbabaie, J. Lin, and A. S. Morse. Coordination of groups of mobile autonomous agents using nearest neighbor rules. *IEEE Trans. on Automatic Control*, 48(6):988–1001, 2003.

[12] M. Ji and M. Egerstedt. Distributed coordination control of multiagent systems while preserving connectedness. *IEEE Trans. on Robotics*, 23(4):693–703, 2007.

[13] H. Kawashima and M. Egerstedt. Approximate manipulability of leader-follower networks. *IEEE Conf. on Decision and Control and European Control Conference*, pages 6618–6623, 2011.

[14] H. Kawashima and M. Egerstedt. Leader selection via the manipulability of leader-follower networks. *American Control Conference*, pages 6053–6058, 2012.

[15] Z. Kira and M. A. Potter. Exerting human control over decentralized robot swarms. *Int. Conf. on Autonomous Robots and Agents*, pages 566–571, 2009.

[16] J. M. McNew, E. Klavins, and M. Egerstedt. Solving coverage problems with embedded graph grammars. *Hybrid Systems: Computation and Control*, pages 413–427, 2007.

[17] M. Mesbahi and M. Egerstedt. *Graph Theoretic Methods in Multiagent Networks*. Princeton University Press, 2010.

[18] N. Michael and V. Kumar. Controlling shapes of ensembles of robots of finite size with nonholonomic constraints. *Robotics: Science and Systems IV*, 2008.

[19] L. Moreau. Stability of multiagent systems with time-dependent communication links. *IEEE Trans. on Automatic Control*, 50(2):169–182, 2005.

[20] P. Ögren, M. Egerstedt, and X. Hu. A control lyapunov function approach to multiagent coordination. *IEEE Trans. on Robotics and Automation*, 18(5):847–851, 2002.

[21] R. Olfati-Saber. Distributed structural stabilization and tracking for formations of dynamic multi-agents. *IEEE Conf. on Decision and Control*, pages 209–215, 2002.

[22] R. Olfati-Saber. Near-identity diffeomorphisms and exponential ϵ-tracking and ϵ-stabilization of first-order nonholonomic SE(2) vehicles. *American Control Conference*, pages 4690–4695, 2002.

[23] A. Rahmani, M. Ji, M. Mesbahi, and M. Egerstedt. Controllability of multi-agent systems from a graph-theoretic perspective. *SIAM Journal on Control and Optimization*, 48(1):162–186,, 2009.

[24] B. Roth. Rigid and flexible frameworks. *The American Mathematical Monthly*, 88(1):6–21, 1981.

[25] H. G. Tanner. On the controllability of nearest neighbor interconnections. *IEEE Conf. on Decision and Control*, pages 2467–2472, 2004.

[26] H. G. Tanner, A. Jadbabaie, and G. J. Pappas. Stable flocking of mobile agents. part ii: Dynamic topology. *IEEE Conf. on Decision and Control*, pages 2016–2021, 2003.

[27] T. Yoshikawa. Manipulability of robotic mechanisms. *The International Journal of Robotics Research*, 4(2):3–9, 1985.

[28] F. Zhang, V. Kumar, and G. A.S. Pereira. Necessary and sufficient conditions for localization of multiple robot platforms. *Proc. the 2004 ASME Design Engineering Technical Conference*, 2A:13–22, 2004.

[29] F. Zhang and N. E. Leonard. Coordinated patterns of unit speed particles on a closed curve. *Systems and Control Letters*, 56(6):397–407, 2007.

A Proof of Lemma 4.3 (the Hessian of Edge-Tension Energy $\mathcal{E}$)

Let $\{v_i, v_j\} \in \mathsf{E}$. The second derivative of $\mathcal{E}_{ij}(x_i, x_j)$ in (4) with respect to x_i in a general configuration of x_i and x_j (i.e., without assuming $||x_i - x_j|| = d_{ij}$) becomes

$$\frac{\partial^2 \mathcal{E}_{ij}(x_i, x_j)}{\partial x_i^2} \left(= -\frac{\partial^2 \mathcal{E}_{ij}(x_i, x_j)}{\partial x_i \partial x_j} \right)$$
$$= \frac{w'_{ij}(||x_i - x_j||)}{||x_i - x_j||}(x_i - x_j)(x_i - x_j)^T + w_{ij}(||x_i - x_j||)I_d,$$

where the equality in the bracket follows from the fact that $\frac{\partial \mathcal{E}_{ij}}{\partial x_i}$ is a function of $x_i - x_j$. Let $e''_{ij}(z) \triangleq \frac{d^2 e_{ij}(z)}{dz^2}$ with $z > 0$,

$$w'_{ij}(z) = \frac{dw_{ij}}{dz} = \frac{\left(e'_{ij}(z)^2 + e_{ij}(z)e''_{ij}(z)\right)z - e_{ij}(z)e'_{ij}(z)}{z^2}.$$

If $||x_i - x_j|| = d_{ij}$, then $e_{ij}(d_{ij}) = 0$, $w_{ij}(d_{ij}) = 0$, and $w'_{ij}(d_{ij}) = \frac{e'_{ij}(d_{ij})^2}{d_{ij}}$. Hence,

$$\frac{\partial^2 \mathcal{E}_{ij}}{\partial x_i^2} = -\frac{\partial^2 \mathcal{E}_{ij}}{\partial x_i \partial x_j} = \left(\frac{e'_{ij}(d_{ij})}{d_{ij}}\right)^2 (x_i - x_j)(x_i - x_j)^T.$$

The matrices $\frac{\partial^2 \mathcal{E}}{\partial x_f^2}$ and $\frac{\partial^2 \mathcal{E}}{\partial x_f \partial x_\ell}$ consist of $N_f \times N_f$ blocks and $N_f \times N_\ell$ blocks, respectively, where each block is $d \times d$ matrix. Specifically,

$$\left[(i,j) \text{ block of } \frac{\partial^2 \mathcal{E}}{\partial x_f^2}\right] = \begin{cases} \sum_{k \in \mathcal{N}(f_i)} \frac{\partial^2 \mathcal{E}_{f_i k}}{\partial x_{f_i}^2} & (i = j) \\ \frac{\partial^2 \mathcal{E}_{f_i f_j}}{\partial x_{f_i} \partial x_{f_j}} = -\frac{\partial^2 \mathcal{E}_{f_i f_j}}{\partial x_{f_i}^2} & (i \neq j) \end{cases}$$

$$\left[(i,j) \text{ block of } \frac{\partial^2 \mathcal{E}}{\partial x_f \partial x_\ell}\right] = \frac{\partial^2 \mathcal{E}_{f_i \ell_j}}{\partial x_{f_i} \partial x_{\ell_j}} = -\frac{\partial^2 \mathcal{E}_{f_i \ell_j}}{\partial x_{f_i}^2},$$

where we used $f_i \triangleq f(i)$ $(i = 1, ..., N_f)$ and $\ell_i \triangleq \ell(i)$ $(i = 1, ..., N_\ell)$ to simplify the notations. Noting that the neighbor set $\mathcal{N}(f_i)$ can include leader agents, from the above equations we obtain $\frac{\partial^2 \mathcal{E}}{\partial x^2}\big|_{x=x^*} = R^T(W')^2 R$, $\frac{\partial^2 \mathcal{E}}{\partial x_f^2}\big|_{x=x^*} = R_f^T(W')^2 R_f$, and $\frac{\partial^2 \mathcal{E}}{\partial x_f \partial x_\ell}\big|_{x=x^*} = R_f^T(W')^2 R_\ell$, where recall that all the desired distances are satisfied at $x = x^*$. $\square$